Extraordinary ^{99}Mo Adsorption: Utilizing Spray-Dried Mesoporous Alumina for Clinical-Grade Generator Development

Azhar Alowasheeir,[1] Miharu Eguchi,[2,3] Yoshitaka Fujita,[*4] Kunihiko Tsuchiya,[4] Ryutaro Wakabayashi,[5] Tatsuo Kimura,[5] Katsuhiko Ariga,[6,7] Kentaro Hatano,[8] Nobuyoshi Fukumitsu,[9] and Yusuke Yamauchi[1,3,6]

[1]Department of Materials Process Engineering, Graduate School of Engineering, Nagoya University, Nagoya 464-8601, Japan
[2]School of Advanced Science and Engineering, Waseda University, Shinjuku-ku, Tokyo 169-8555, Japan
[3]Australian Institute for Bioengineering and Nanotechnology (AIBN), The University of Queensland, Brisbane, Queensland 4072, Japan
[4]Department of JMTR, Japan Atomic Energy Agency, 4002 Narita, Oarai, Ibaraki 311-1393, Japan
[5]National Institute of Advanced Industrial Science and Technology (AIST), Sakurazaka, Moriyama-ku, Nagoya 463-8560, Japan
[6]Research Center for Materials Nanoarchitectonics (MANA), National Institute for Material Science, 1-1 Namiki, Tsukuba, Ibaraki 305-0044, Japan
[7]Graduate School of Frontier Sciences, The University of Tokyo, Kashiwa, Chiba 277-0827, Japan
[8]Department of Applied Molecular Imaging, Faculty of Medicine, University of Tsukuba, 1-1-1 Tennodai, Tsukuba, Ibaraki 305-8575, Japan
[9]Department of Radiation Oncology, Kobe Proton Center, 1-6-8 Minatojima-Minamimachi, Chuo-ku, Kobe, Hyogo 605-0047, Japan

*Corresponding author: Department of JMTR, Japan Atomic Energy Agency, 4002 Narita, Oarai, Ibaraki, 311-1393. Email: fujita.yoshitaka@jaea.go.jp

Yoshitaka Fujita
Yoshitaka Fujita was assigned to department of JMTR, Japan Atomic Energy Agency (JAEA) in 2015. His research focuses on development of Mo adsorbents used for medical ^{99}Mo/^{99m}Tc generators. He received his Ph.D. from Nagaoka University of Technology in 2022. Currently, He is involved in Ac-225 production development at the experimental fast reactor Joyo.

Abstract

Mesoporous alumina spherical particles, synthesized *via* spray-drying with the self-assembly of $EO_nPO_mEO_n$, have been utilized for the development of clinical-grade molybdenum-99/technetium-99m (^{99}Mo/^{99m}Tc) generators. When evaluated as molybdenum (Mo) adsorbents, the mesoporous alumina spherical particles are useful for effective adsorption of molybdenum ions rather than commercially available particulate alumina. The effects of surfactant removal methods on the Mo adsorption property are also systematically investigated using the batch method. Batch adsorption studies reveal practical adsorption capacities ranging from 45.9 to 91.2 mg Mo/g in a Mo solution (1000 mg-Mo/L) at pH 3. The experimental results indicate the following trend in Mo adsorption capacity: solvent extraction > calcination (400 °C and 800 °C) > commercially available alumina (Medical Al_2O_3 used as is). To explore the feasibility of developing a clinical-scale generator, a novel tandem column generator concept is employed. Using the spray-dried and extracted mesoporous alumina, ^{99m}Tc eluted from the generator exhibits high radionuclidic, radiochemical, and chemical purity, making it suitable for the preparation of ^{99m}Tc-labeled radiopharmaceuticals.

Keywords: Alumina, ^{99}Mo/^{99m}Tc generators, Mo adsorbent

Graphical abstract

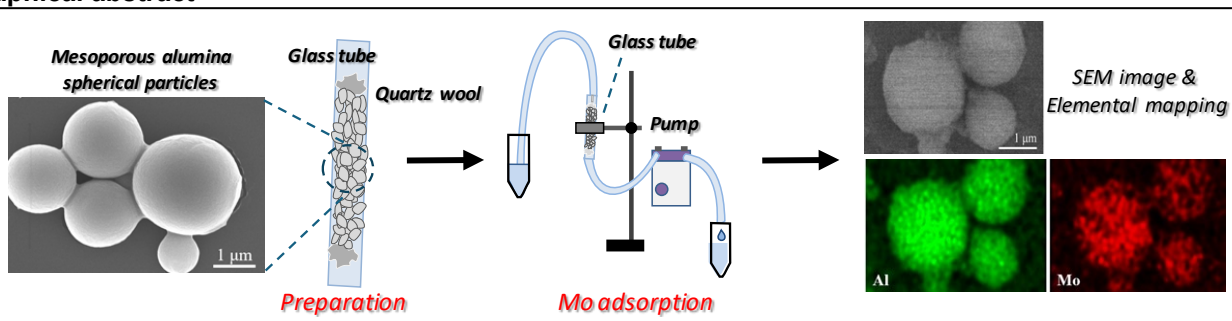

Mesoporous alumina spherical particles, synthesized via spray-drying with the self-assembly of $EO_nPO_mEO_n$, have been utilized for the development of clinical-grade ^{99}Mo/^{99m}Tc generators. ^{99m}Tc eluted from the generator exhibits high radionuclidic, radiochemical, and chemical purity, making it suitable for the preparation of ^{99m}Tc-labeled radiopharmaceuticals.

1. Introduction

The use of radiopharmaceuticals in nuclear medicine is an indispensable tool in modern medical diagnostics.[1-3] According to the latest survey published in 2023,[4] in our country, technetium-99m (^{99m}Tc) is used in an average of 682,430 examinations annually. This is the highest figure among all radioactive isotopes. Fluorine-18 (^{18}F) used in positron emission tomography (PET) (with 612, 909 examinations annually) closely follows ^{99m}Tc, but the number of PET facilities is still limited. Therefore, ^{99m}Tc is overwhelmingly the most frequently used single-photon emitting isotope available in many medical facilities. ^{99m}Tc is used for the diagnosis of conditions such as dementia, cerebral infarction, pulmonary embolism, myocardial infarction, bone metastasis, lymph node metastasis, and renal dysfunction, accounting for over 60% of all examinations using single-photon emission isotopes.

^{99m}Tc is characterized as a radiopharmaceutical suitable for nuclear medicine examinations due to its emission of a γ-ray with an energy of 140 keV and a short half-life of 6 hours.[5,6] ^{99m}Tc is generated from its parent nuclide, ^{99}Mo (half-life: 66 hours). The production of ^{99}Mo is mainly obtained by irradiating ^{235}U with thermal or fast neutrons. All ^{99}Mo is imported from other countries, Therefore, supply shortages occur every few years due to various situations overseas, significantly impacting medical systems. 99Mo can also be obtained by irradiating natural Mo, but because of the large amount of other Mo isotopes present, this method requires the adsorption of more Mo to obtain a sufficient amount of ^{99m}Tc.[7] Current commercial ^{99}Mo/^{99m}Tc generators typically have an adsorption capacity of 2 to 20 mg Mo g^{-1} alumina[8], but our calculations suggest that an adsorption capacity of around 200 mg Mo g^{-1} is needed to obtain ^{99m}Tc from the irradiation of natural Mo. Therefore, the development of alumina absorbents with improved ^{99}Mo adsorption capacity is extremely important. Extensive research has been conducted in recent years to address this need, including the exploration of advanced materials.[9-12] Cecilia C. Guedes-Silva et al. achieved the adsorption of Mo at 92.45 mg Mo per g alumina by calcinating alumina at 900 °C for 5 hours, resulting in the presence of θ and γ-Al_2O_3 with a high specific surface area (153.7 m^2 g^{-1}).[13]

Our objective is to advance the field of nuclear medicine by exploring various alumina-based sorbents. In the previous reports, mesoporous/nanoporous alumina materials with various structural and compositional decorations have been synthesized to achieve high Mo adsorption performance.[14-16] Building on previous knowledge, which demonstrated that Mo ions interact with surface hydroxyl (Al-OH) groups,[17] our goal in this study is to retain a large number of Al-OH groups for maximizing the amount of adsorbed Mo ions. As a model study, we investigate the effect of adsorbed Mo amount using mesoporous alumina prepared through different surfactant removal methods (*i.e.*, solvent extraction method, and calcination methods at different temperatures). The extracted mesoporous alumina with a sufficient amount of Al-OH groups exhibits 82.6 mg g^{-1} of Mo adsorption. To investigate the feasibility of developing a clinical-scale generator, we employ a novel tandem column generator concept. By utilizing the spray-dried and extracted mesoporous alumina, we achieve a high radionuclidic, radiochemical, and chemical purity in the eluted ^{99m}Tc from the generator. This makes it suitable for the preparation of ^{99m}Tc-labeled radiopharmaceuticals.

2. Experimental

Materials

Aluminum tri-*sec*-butoxide ($Al(OsBu)_3$) was obtained from Kanto Chemical Co., Inc. Concentrated aqueous hydrochloric acid (conc. HCl, 35-37 wt%), ethanol (EtOH) and triethylamine (Et_3N), 6 M NaOH solution, 2 M HCl solution and camphor was obtained from Fujifilm Wako Pure Chemical Corporation. Pluronic P123 ($EO_{20}PO_{70}EO_{20}$) was purchased from Sigma-Aldrich. MoO_3 powder was purchased from Taiyo Koko Co., Ltd., 99.99 %. 5 M sodium chloride solution was purchased from Nacalai Tesque Inc. Commercially available medical alumina powders (hereafter abbreviated as Medical Al_2O_3) (MP Alumina R for isotope, acid pH, 63-200 μm) were also purchased as comparison samples.

Spray-dried mesoporous alumina:

Spherical particles of high-surface-area mesoporous alumina can be prepared by spray-drying precursor solutions containing aluminum alkoxides with a rational approach to improve the connectivity of $EO_nPO_mEO_n$ templated mesopores.[18,19] Referring to our previous paper utilizing Al(OsBu) a clear ethanolic precursor solution was prepared as follows and spray-dried at an inlet temperature of 170 ºC.[19] $Al(OsBu)_3$ (10 mmol, 24.6 g) was dispersed in EtOH, (60 mL) followed by a dropwise addition of conc. HCl solution. After stirring for 3 hr at room temperature, the resultant solution containing pre-hydrolyzed aluminum species was combined with another ethanolic solution of Pluronic P123 ($EO_{20}PO_{70}EO_{20}$, 15 g in 120 mL of EtOH). The resultant powder sample was calcined at 400 ºC and 850 ºC (named as "Al_2O_3_400" and "Al_2O_3_850", respectively). Our neutralization-mediated extraction process was also applied for removing Pluronic P123, which was assisted by organic bases such as Et_3N as a scavenger of residual HCl and stabilizer of alumina framework.[20] The advantage of solvent extraction is the retention of abundant Al-OH groups, preventing thermal condensation between Al-OH groups. The resultant powder sample (0.5 g) was added to an ethanolic solution containing 0.1 M Et_3N (10 mL), mixed for 1 h at room temperature, and recovered by vacuum filtration (named as "Extracted Al_2O_3").

Characterization:

The phase purity of the samples was confirmed by powder X-ray diffraction (PXRD) using a Rigaku RINT Ultima III diffractometer (Cu Kα radiation, 40 kV and 40 mA) at a scanning rate of 10 ° min^{-1}. The XRD data were collected in the 2θ range of 10–90° under ambient conditions. A small-angle X-ray scattering (SAXS) Rigaku MicroMax-007H was employed to obtain the mesostructural periodicity of the samples. The morphological characterization of the samples was conducted using a Hitachi SU8000 scanning electron microscope (SEM) operating at an accelerating voltage of 5

kV. N_2 adsorption-desorption isotherms of the samples were measured on a Quantachrome Autosorb gas sorption system (Anton Paar) at 77 K. Before the measurement, the samples were treated at 100°C for 24 hours. Fourier Transform Infrared Spectroscopy (FT-IR) was carried out on a JASCO FTIR-4100 using the potassium bromide (KBr) pellet method, where the alumina sample (0.5 mg) was mixed with KBr (100 mg) for qualitative evaluation. The sample was stored in dry atmospheres without heating before measurement.

Preparation of ^{99}Mo solution.

The typical preparation of the sodium molybdenum solution involved dissolving 75 mg of MoO_3 powder in 1.74 mL of 6 M NaOH solution. The solution's pH was then carefully adjusted to 3 by slowly adding 2 M HCl solution. After pH adjustment, deionized water was added gradually until the molybdenum concentration reached the desired endpoint of 1000 mg Mo L^{-1}, thus creating the solution for further analytical procedures.

Evaluation of molybdenum adsorption capacity.

0.07 g of each Al_2O_3 sample was mixed with 7 mL of the above-prepared Mo solution. The mixture was then gently agitated for 2 hours at room temperature. Afterward, the mixture was filtered through a 0.2 μm filter. The remaining Al_2O_3 was washed with deionized water. Meanwhile, the filtrate containing the Mo solution was combined with the rinse fluid from the Al_2O_3 and used for Mo concentration analysis. The Mo adsorption capacity was calculated by subtracting the measured Mo concentration from the initially added concentration.

Mo adsorption/^{99m}Tc elution.

The MoO_3 pellets were fabricated by blending MoO_3 powder with 2 wt% camphor and ethanol, then the mixture was shaped into pellets using a uniaxial press. These moldings underwent sintering at 650 °C. Once adequately dried, the MoO_3 pellets were roughly crushed, with approximately 1.5 g utilized for neutron irradiation. Neutron irradiation of the MoO_3 pieces occurred at 5 MW for 20 min, utilizing the irradiation orifice of pneumatic tube Pn-2 from the Kyoto University Research Reactor (KUR). After irradiation, the MoO_3 pieces were allowed to decay for 4 days before being utilized in experiments. Subsequently, the irradiated MoO_3 pieces were dissolved in a 6 M NaOH aqueous solution. The pH of the solution was adjusted to 3 by titrating with 2 M HCl solution, and the Mo concentration was adjusted to 20 g Mo L^{-1} by diluting with deionized water. This resulting solution, termed the Mo solution, was then employed for Mo adsorption and ^{99m}Tc elution property evaluations. In the experiment, a glass tube with an inner diameter of 4.2 mm was filled with 0.07 g of alumina specimen for further testing. The setup involved fixing the alumina specimen within the tube using upper and lower quartz wool. The alumina bed heights were approximately 8 mm. This alumina column was then connected to a peristaltic pump, through which 1 ml of Mo solution was passed. The flow rates were 4.29 mL min^{-1} and 2.31 mL min^{-1} for Extracted Al_2O_3 and Medical Al_2O_3, respectively. Subsequently, 10 mL of saline solution was passed through the column to remove any remaining ^{99m}Tc and ^{99}Tc. The saline solution was prepared as a 0.90 % w/v solution of NaCl using 5 M sodium chloride solution. The activities of ^{99}Mo in both the Mo solution and the saline solution after passing through the column were measured. Following a 24 h interval, the column underwent a milking procedure. In this step, 1 mL of saline was passed through the column five times, totaling 5 mL, to assess the elution properties of ^{99m}Tc. The flow rates were 1.08 mL min^{-1} and 2.90 mL min^{-1} for Extracted Al_2O_3 and Medical Al_2O_3, respectively.

The activities of both ^{99}Mo and ^{99m}Tc in the resulting ^{99m}Tc solution were determined. These activities were measured using a γ-ray spectrometer manufactured by Mirion Technologies (Canberra) KK. To calculate the Mo adsorption capacity of the alumina specimen, the Mo content in the solution after adsorption was subtracted from the Mo content in the solution before adsorption. The Mo adsorption capacity, expressed in milligrams of Mo per gram of alumina (mg Mo g^{-1}), was calculated based on the specific activity of ^{99}Mo at the beginning of the adsorption process.

3. Results and discussion

The SEM images (**Fig. S1a**) confirm the formation of spherical particles of as-synthesized Al_2O_3, which is typical for samples recovered by the spray-drying process of a precursor solution. The extracted sample and those calcined at two different temperatures (400 °C and 850 °C) retain the original spherical morphology (**Fig. 1a-c**). Notably, the morphology is maintained even after undergoing the high-temperature calcination (850 ºC). For reference, the SEM image and wide-angle XRD pattern of Medical Al_2O_3 show irregular shapes consisting of aggregated particles. (**Fig. S1b** and **S2**).

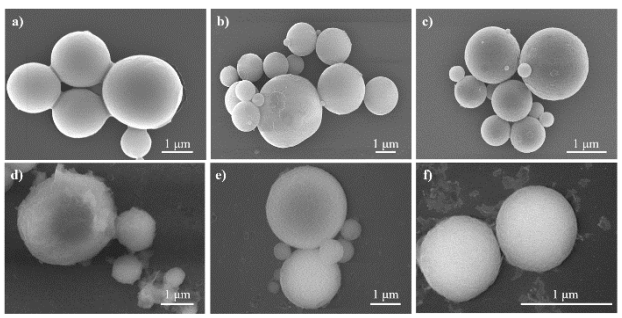

Fig. 1. (a-c) SEM images of (a) Extracted Al_2O_3 (b) Calcined Al_2O_3_400 and (c) Calcined Al_2O_3_850 before Mo adsorption. (d-f) SEM images of (d) Extracted Al_2O_3 (e) Calcined Al_2O_3_400 and (f) Calcined Al_2O_3_850 after Mo adsorption.

To validate the periodicity of the $EO_nPO_mEO_n$ templated mesopores and investigate the crystal structure, both low-angle and wide-angle XRD measurements were carried out. The low-angle XRD patterns of the samples (**Fig. 2a**) exhibit an obvious single peak, indicating the periodic arrangement of the mesopores. The *d*-spacings of Extracted Al_2O_3, Calcined Al_2O_3_400, and Calcined Al_2O_3_850 were measured to be 7.4 nm, 6.1 nm, and 5.3 nm, respectively. After calcination, the framework is solidified by condensation of Al-OH groups, resulting in a reduction of the mesostructural periodicity. Further increasing the calcination

temperature up to 850 °C reduces the *d*-spacing to support the condensation between the Al-OH groups to proceed with alumina framework shrinkage.

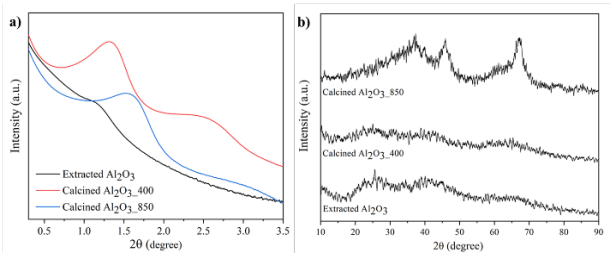

Fig. 2. (a) Low-angle XRD patterns and (b) wide-angle XRD patterns of (i) Extracted Al_2O_3, (ii) Calcined Al_2O_3_400, and (iii) Calcined Al_2O_3_850.

Meanwhile, the wide-angle XRD patterns (**Fig. 2b**) suggest a transition to the γ- phase of Al_2O_3 as the calcination temperature increases. In the wide-angle XRD patterns, both the extracted and calcined (at 400 °C) samples display broad peaks, indicating the presence of amorphous Al_2O_3.[21] Following calcination at 850 °C, small diffraction peaks emerge at $2\theta = 45.74$ and 66.96º, corresponding to the (400) and (440) planes of γ-Al_2O_3, respectively.[22] Although the crystallinity is modest, a polycrystalline alumina framework is formed. The average crystallite size, calculated from the full width at half-maximum of the (400) peak at $2\theta = 45.74$º, is approximately 0.87 nm. Thus, the heat treatment at 850 °C initiates the transformation from amorphous to γ-Al_2O_3.

The N_2 adsorption-desorption isotherms of the samples are shown in **Fig. 3**. The specific surface areas and pore volumes are summarized in **Table 1**. Extracted Al_2O_3 shows a lower surface area of 180.4 m^2 g^{-1} due to a small amount of remaining carbon content after the extraction process (The remaining carbon content is around 3.7 wt.% by CHN analysis.[20]). Therefore, the pore size distribution curve does not show a clear peak. Although the carbon content is significantly reduced by the extraction process compared to the as-prepared sample, we expect that some fragments of $EO_nPO_mEO_n$ remain in the extracted mesoporous alumina. Since the Japanese Minimum Requirements for Radiopharmaceuticals (MRRP) specify only Al, the influence of the remaining P123 was not evaluated in this study. However, due to medical applications, confirming its effect remains a future challenge.

It is noteworthy that the specific surface area increases following heat treatment. However, Calcine d Al_2O_3_850 exhibits a lower surface area (341 m^2 g^{-1}) compared to Calcined Al_2O_3_400 (449 m^2 g^{-1}). The reduction of specific surface area by calcination at 850 °C is attributable to the collapse of the mesoporous structure with thermal condensation of Al-OH groups and following alumina grain growth. This is supported by a significant reduction of the primary peaks (**Fig. 2a**).

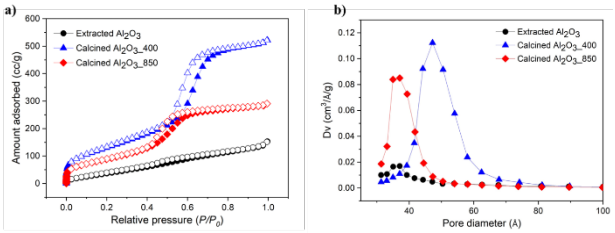

Fig. 3. (a) N_2 adsorption-desorption isotherms, and (b) BJH pore size distribution curves of Extracted Al_2O_3, Calcined Al_2O_3_400, and Calcined Al_2O_3_850.

The pH of the solution influences on adsorption of ^{99}Mo, as it affects the difference molybdenum species present[23] and the surface charge of the adsorbents.[24] Where $Mo_7O_{24}^{3-}$ is dominant at < pH 2, while both $Mo_7O_{24}^{6-}$ and $Mo_8O_{28}^{4-}$ exist at pH 2-5, and MoO_4^{2-} predominates at > pH 6.[25] Previous reports demonstrated a study on the distribution ratios (K_d) to assess the potential use of the synthesized sorbent for the radiochemical separation of ^{99m}Tc from ^{99}Mo at various pHs.[26] It was observed that at pH 3, the K_d value of molybdate ions was the highest. This phenomenon was attributed to the presence of hydroxyl groups on the surface of Al_2O_3, which became protonated, resulting in a positively charged surface that attracts $Mo_7O_{24}^{6-}$ ions.[14] Based on these findings, Mo solutions with a pH of 3 were prepared in the experimental section of this study. The adsorption capacities of different Al_2O_3 samples were determined using batch equilibration methods (static) in 4 different batches. When the alumina samples were mixed with Mo solution, the solution became cloudy except for Medical Al_2O_3. Therefore, it is estimated that the alumina samples prepared in this study have finer grain size than Medical Al_2O_3. The Mo adsorption capacities obtained from all samples are shown in **Table 1**. The extracted Al_2O_3 exhibits the highest adsorption capacity of 91.2 mg Mo/g, surpassing other Al_2O_3 samples. The experimental results indicate the following trend in Mo adsorption capacity: solvent extraction method > calcination method (at 400 °C and 800 °C) > Medical Al_2O_3. SEM images in **Fig. 1d-f** show that the morphology of all the Al_2O_3 samples remains unaltered even after Mo adsorption, although the surface of the particles becomes slightly bumpy with some flakes appearing. Energy-dispersive X-ray spectroscopy (EDX) confirms a uniform distribution of aluminum (Al) and adsorbed molybdenum (Mo) throughout

Table 1. Summary of surface areas, pore volumes, and Mo adsorption capacity of alumina samples (Extracted as-prepared sample, two calcinated samples at different temperatures (400 and 850 °C), and commercially available Medical Al_2O_3 sample.).

Sample names	Surface area (m^2 g^{-1})	Pore Volume (cm g^{-1})	Mo adsorption capacity (mg Mo g^{-1})
Extracted Al_2O_3	180.4	0.21	91.2
Calcined Al_2O_3_400	499.4	0.85	45.9
Calcined Al_2O_3_850	340.8	0.47	48.8
Medical Al_2O_3	115.0	0.23	35.5

the entire area, as revealed by corresponding elemental mapping images in Fig. 4.

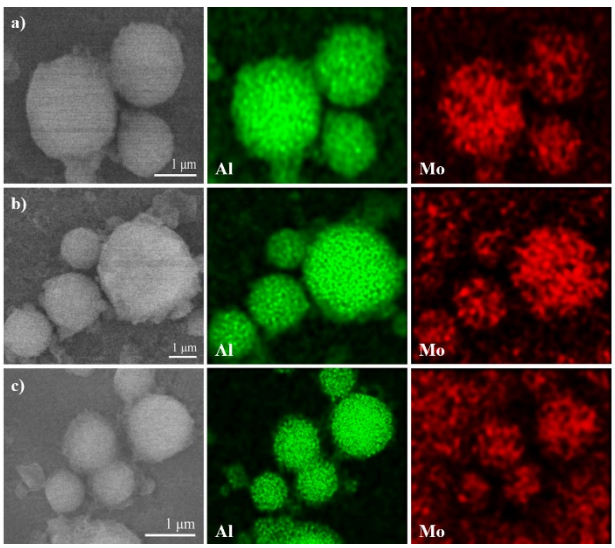

Fig. 4. SEM images and EDX mapping of (a) Extracted Al_2O_3 (b) Calcined Al_2O_3_400 and (c) Calcined Al_2O_3_850 after Mo adsorption.

As discussed above, the presence of hydroxyl groups plays a significant role in the adsorption of ^{99}Mo, as demonstrated in previous reports.[17] To investigate this point, the existence of hydroxyl groups on the Extracted Al_2O_3 and Medical Al_2O_3 before the adsorption process was confirmed using FTIR. In order to compare the amount of OH groups, the alumina samples were thoroughly dried in a dry atmosphere without heating. In **Fig. 5**, a broad peak is observed at 3600-3200 cm^{-1} and around 1635-1622 cm^{-1}, corresponding to OH stretching groups.[27] The intensity of these peaks indicates the quantity of OH groups present, with the intensity of OH groups being higher in the Extracted Al_2O_3 than in Medical Al_2O_3. A large number of OH groups enhance Mo adsorption due to the strong interaction between protonated OH groups on the surface of Al_2O_3 and negatively charged Mo species at pH=3.[17] In our previous study,[20] from thermogravimetry differential thermal (TG-DTA) analysis, it was revealed that many –OH groups were present in the extracted sample, significantly more than in the mesoporous (still amorphous) alumina obtained by direct calcination at 400°C. This result is related to the room-temperature extraction process being very mild, thus avoiding the condensation of surface –OH groups.

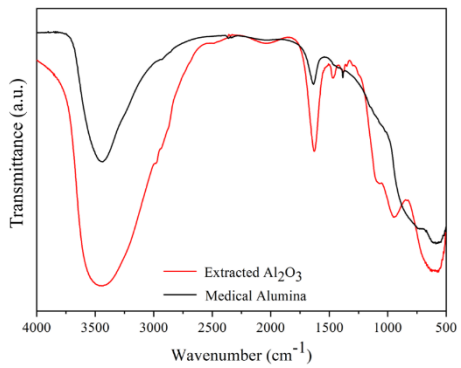

Fig. 5. FTIR of Extracted Al_2O_3 and Medical Al_2O_3. The same amount of samples was measured by FTIR to compare the relative abundance of hydroxyl groups (-OH) on the surfaces of Extracted Al_2O_3 and Medical Al_2O_3.

Extracted Al_2O_3 was chosen for Mo adsorption and elution of ^{99m}Tc due to its demonstrated high Mo adsorption capacity. For comparison, commercial Medical Al_2O_3 was also utilized in this study. The radioactivity of ^{99}Mo was calculated using the Covell method from the energy of 0.739 MeV, as specified in MRRP (**Scheme 1**). The specific radioactivity of ^{99}Mo upon adsorption is determined to be 22.9 MBq/g Mo. The ^{99}Mo adsorption capacity of Extracted Al_2O_3 is calculated to be 1.90 MBq ^{99}Mo g^{-1} Al_2O_3. Converting the Mo adsorption capacity using the specific

Table 2. Summary of analyzing milking metrics with Extracted Al_2O_3 and Medical Al_2O_3.

	Extracted Al_2O_3 Activity on the column at the start of milking： ^{99m}Tc 93.5kBq, ^{99}Mo 106.1kBq					**Medical Al_2O_3** Activity on the column at the start of milking： ^{99m}Tc 45.6kBq, ^{99}Mo 52.1kBq				
Accumulated elute volume (mL)	**0.711**	**1.786**	**2.734**	**3.679**	**4.951**	**0.989**	**1.963**	**2.985**	**3.863**	**5.034**
Activity of ^{99m}Tc (kBq)	24.8	45.3	50.5	52.6	54.0	24.4	27.8	28.1	28.1	28.1
Total elution ratio of ^{99m}Tc (%)	26.5	48.5	54.0	56.2	57.8	53.4	60.9	61.6	61.7	61.7
Activity of ^{99}Mo (kBq)	below detection limit*	below detection limit*	below detection limit*	below detection limit*	below detection limit*	3.24	4.19	4.19	4.19	4.65
^{99}Mo/^{99m}Tc (%)	0	0	0	0	0	13.3	15.1	14.9	14.9	16.5
pH	4.42					4.53				

*Based on the literature (Nuclear Instruments and Methods, 82 (1970) 273-277), detection limits were calculated and ^{99}Mo was non-detectable.

activity of ^{99}Mo upon adsorption yielded 82.6 mg Mo g^{-1} Al_2O_3. This value is noteworthy when compared to the current limit of use in ^{99}Mo/^{99m}Tc generators which is typically from 2 to 20 mg Mo g^{-1} Al_2O_3.[8] On the other hand, the ^{99}Mo adsorption capacity by Medical Al_2O_3 is 22.6 MBq g^{-1} Mo. When the Mo adsorption capacity is recalculated using the specific activity of ^{99}Mo upon adsorption, it results in 41.3 mg Mo g^{-1} Al_2O_3. The Extracted Al_2O_3 thus exhibits approximately twice the Mo adsorption capacity of Medical Al_2O_3. The radioactivity of ^{99}Tc is determined to be 0.141 MeV by using the Covell method, as specified in MRRP for the radioactivity of ^{99m}Tc from the energy peak. **Fig. 6a** and **Table 2** show the total ^{99m}Tc elution ratio by Extracted Al_2O_3 and Medical Al_2O_3. The vertical axis represents the ratio of the activity of ^{99m}Tc present on the alumina column at the start of milking to the activity of eluted ^{99m}Tc. The ratios for Extracted Al_2O_3 and Medical Al_2O_3 are saturated (57.8% and 61.7%, respectively) with 5 mL of milking. Since the elution ratios for both are about 60%, these results are probably due to the effects of column size. In this experiment, the column is too small to control the flow rate. The ratios can be improved by increasing the column size and setting the appropriate flow rate. Both eluted ^{99m}Tc solutions are clear and colorless. Because ^{99m}Tc solution is injected into the body as a radiopharmaceutical, MRRP defined the standard pH value of ^{99m}Tc solutions to be pH 4.5 to 7.0. The pH of the ^{99m}Tc solution obtained from Extracted Al_2O_3 is pH 4.4, which is a lower limit of the pH standard value, but an improvement can be expected by increasing the liquid volume. The pH of the ^{99m}Tc solution obtained from Medical Al_2O_3 (4.5) is within the standard range of values. In MRRP, the amount of ^{99}Mo desorbed in a ^{99m}Tc solution is defined using the ^{99}Mo/^{99m}Tc ratio as an index and the standard value for ^{99}Mo/^{99m}Tc is less than 0.015 %.

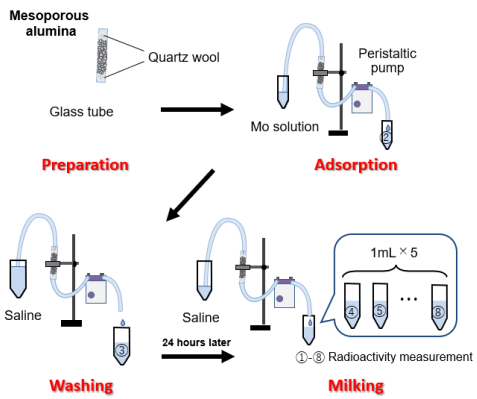

Scheme 1. Procedure of milking test.

Fig. 6b and **Table 2** show the ^{99}Mo/^{99m}Tc ratio in the ^{99m}Tc solution after the milking test. The ^{99}Mo concentration obtained from Extracted Al_2O_3 is below the detection limit (*i.e.*, 0 % in Table 2) and meets the standard value for the ^{99}Mo/^{99m}Tc ratio. On the other hand, the ^{99}Mo/^{99m}Tc ratio obtained from Medical Al_2O_3 is 13.3-16.5 %, which exceeds the standard value specified in MRRP. These results suggest that the amount of -OH group significantly influences both Mo adsorption and ^{99m}Tc elution. The pH of the final solution after the milking test is almost within the standard pH range defined by MRRP.

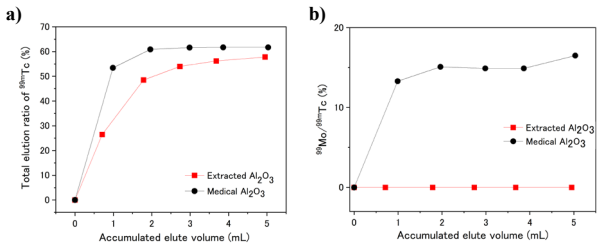

Fig. 6. (a) The ^{99m}Tc elution properties and (b) ^{99}Mo/^{99m}Tc ratio in the ^{99m}Tc solution, obtained by extracted and Medical Al_2O_3.

4. Conclusion

The high specific surface area as well as the presence of abundant surface -OH group on Extracted Al_2O_3 are helpful for exceptional Mo adsorption and ^{99m}Tc elution at low pH value, highlighting its potential for developing more efficient and scalable ^{99}Mo/^{99m}Tc generators compared to commercial Medical Al_2O_3. Further optimization and scale-up of the synthesis process can enhance its applicability in nuclear medicine diagnostics, addressing the growing clinical demand for ^{99m}Tc.

Acknowledgement

The authors acknowledge Mr. Y. Fujihara, Mr. H. Yoshinaga, and Prof. J. Hori for supporting the irradiation experiments at the KUR.

Supplementary data

Supplementary material is available at *Bulletin of the Chemical Society of Japan.*

Funding

This work was supported by JSPS KAKENHI Grant Number JP22H03974.

Conflict of interest statement. None declared.

References

1 A. Boschi, L. Uccelli, L. Marvelli, C. Cittanti, M. Giganti, P. Martini, *Molecules* **2022**, *27*, 1188.
2 M. Riondato, D. Rigamonti, P. Martini, C. Cittanti, A. Boschi, L. Urso, L. Uccelli, *J. Med. Chem*. **2023**, *66*, 4532.
3 I. G. T. Baeten, J. P. Hoogendam, B. Jeremiasse, A. J. A. T. Braat, W. B. Veldhuis, G. N. Jonges, I. M. Jürgenliemk-Schulz, C. H. van Gils, R. P. Zweemer, C. G. Gerestein, *Cancer Rep*. **2022**, *5*, e1401.
4 Y. Nishiyama, A. Okizaki, Y. Inui, H. Otsuka, K. Takanami, M. Nakajo, K. Nakatani, M. Nogami, K. Hirata, Y. Maeda, M. Yoshimura, H. Wakabayashi, *Radioisotopes* **2023**, *72*, 49. (in Japanese)
5 W. C. Eckelman, *JACC Cardiovasc Imaging* **2009**, 2, 364.
6 O. K. Hjelstuen, *Analyst* **1995**, *120*, 863.
7 S. Hasan, M. A. Prelas, *SN Appl. Sci*. **2020**, *2*, 1782.
8 H. Arino, H. H. Kramer, *Int. J. Appl. Radiat. Isot*. **1975**, *26*, 301.
9 D. Das, *ChemRxiv* **2024**.10.26434/chemrxiv-2024-jg1wl

10 N. Takahashi, M. Fujiwara, M. Kurosawa, M. Tamura, Y. Kosuge, T. Kubota, N. Abe, T. Takahashi, *J. Radioanal. Nucl. Chem*. **2024**, *333*, 17.

11 Y. Suzuki, T. Kitagawa, Y. Namekawa, M. Matsukura, K. Nishikata, H. Mimura, K. Tsuchiya, *Trans. Mater. Res. Soc. Jpn*. **2018**, *43*, 75.

12 Y. Fujita, M. Seki, T. Sano, Y. Fujihara, T. Kitagawa, M. Matsukura, J. Hori, T. Suzuki, K. Tsuchiya, *J. Radioanal. Nucl. Chem*. **2021**, *327*, 1355.

13 C. C. Guedes-Silva, T. D. S. Ferreira, F. M. S. Carvalho, C. M. de Paula, L. Otubo, *Mater. Res. Ibero-Am. J. Mater*. **2016**, *19*, 791.

14 I. Saptiama, Y. V. Kaneti, Y. Suzuki, K. Tsuchiya, N. Fukumitsu, T. Sakae, J. Kim, Y. M. Kang, K. Ariga, Y. Yamauchi, *Small* **2018**, *14*, 1800474.

15 D. P. Benu, J. Earnshaw, A. Ashok, K. Tsuchiya, I. Saptiama, B. Yuliarto, V. Suendo, R. R. Mukti, N. Fukumitsu, K. Ariga, Y. V. Kaneti, Y. Yamauchi, *Bull. Chem. Soc. Jpn*. **2021**, *94*, 502.

16 I. Saptiama, Y. V. Kaneti, H. Oveisi, Y. Suzuki, K. Tsuchiya, K. Takai, T. Sakae, S. Pradhan, M. S. A. Hossain, N. Fukumitsu, K. Ariga, Y. Yamauchi, *Bull. Chem. Soc. Jpn*. **2018**, *91*, 195.

17 Y. Fujita, T. Niizeki, N. Fukumitsu, K. Ariga, Y. Yamauchi, V. Malgras, Y. V. Kaneti, C.-H. Liu, K. Hatano, H. Suematsu, T. Suzuki, K. Tsuchiya, *Bull. Chem. Soc. Jpn*. **2022**, *95*, 129.

18 H. Maruoka, A. Tomita, L. Zheng, T. Kimura, *Langmuir* **2018**, *34*, 13781.

19 H. Maruoka, T. Kimura, *New J. Chem*. **2019**, *43*, 7269.

20 R. Wakabayashi, T. Kimura, *Chem. Commun*. **2024**, *60*, 3519.

21 K. Atrak, A. Ramazani, S. Taghavi Fardood, *J. Mater. Sci.: Mater. Electron*. **2018**, *29*, 8347.

22 R. Chakravarty, R. Ram, R. Mishra, D. Sen, S. Mazumder, M. R. A. Pillai, A. Dash, *Ind. Eng. Chem. Res*. **2013**, *52*, 11673.

23 L. Zeng, C. Y. Cheng, *Hydrometallurgy* **2009**, *98*, 10.

24 E. Hayek, *Chromatogr. Rev*. **1960**, *2*, 171.

25 H. Sepehrian, S. Waqif-Husain, J. Fasihi, M. K. Mahani, *Sep. Sci. Technol*. **2010**, *45*, 421.

26 R. Chakravarty, R. Ram, A. Dash, M. R. A. Pillai, *Nucl. Med. Biol*. **2012**, *39*, 916.

27 J. Yu, Y. Le, B. Cheng, *RSC Adv*. **2012**, *2*, 6784